journal

J. Am. Ceram. Soc., **83** [10] 2521–28 (2000)

Tensile Transformation-Mismatch Plasticity of Bismuth Sesquioxide

David C. Dunand[†] and Jeffrey L. Grabowski[*,‡]

Department of Materials Science and Engineering, Northwestern University, Evanston, Illinois 60208

This study reports on experiments where bismuth sesquioxide (Bi_2O_3) was cycled between its high-temperature δ-phase and one or more of its low-temperature phases (α-, β-, or γ-Bi_2O_3) while being subjected to uniaxial tensile stresses in the range of 0.11–0.55 MPa. Reproducible strain increments of 0.4%–3.9% have been measured after each thermal cycle, and total tensile fracture strains of 10%–28% have been obtained using a combination of isothermal creep and transformation-mismatch plasticity. The strain due to transformation mismatch plasticity has been determined by two different methods and is proportional to the applied stress, which is quantitatively consistent with theoretical predictions for transformation superplasticity.

I. Introduction

SUPERPLASTICITY, which is defined as the ability of crystalline materials to deform in tension up to very large strains (typically >100%), can be divided into two categories, based on the deformation mechanisms: microstructural superplasticity and internal-stress superplasticity.[1] The former type relies on grain-boundary sliding at constant temperature and has been reported in ceramics with stable grains less than ~1 μm in size.[1,2] Conversely, internal-stress superplasticity occurs via an accumulation of strain increments during thermal cycling and is independent of grain size. Each strain increment is produced when internal mismatch stresses within the material are relaxed under the effect of an external biasing stress. These internal stresses are produced during a temperature change by a volume mismatch, because of thermal expansion or allotropic transformation between grains in single-phase materials or between phases in composites. Although many metals, alloys, and metal-matrix composites have been reported to deform by internal-stress superplasticity when subjected to thermal cycling,[1,3,4] this phenomenon has not been demonstrated yet for ceramics.

Among allotropic ceramics, one of the best candidates for transformation-mismatch superplasticity is bismuth sesquioxide (Bi_2O_3), because of its low transformation temperature of 730°C (which is high in comparison to its melting temperature, 824°C[5]), the large allotropic volume mismatch of 6.9% between its low-temperature α-phase and its high-temperature δ-phase,[6] and the high creep ductility of the δ-Bi_2O_3 phase.[7,8] Early experiments indeed have shown that a plastic increment could be produced on crossing the allotropic range of pure Bi_2O_3,[9,10] Bi_2O_3–Sm_2O_3 eutectoids,[10,11] and the related oxides Bi_2WO_6 and Bi_2MoO_6.[9,12] However, this transformation-mismatch plasticity cannot be called transformation superplasticity, because deformation was observed only in compression and was not repeatable on multiple cycles.

The interest in achieving transformation-mismatch superplasticity in Bi_2O_3 is two-fold. First, δ-Bi_2O_3 is an intrinsic fast-ion conductor with applications for solid oxide fuel cells, batteries, sensors, and electrochemical pumps.[13,14] The complex Bi_2O_3 shapes that are necessary for such devices can be achieved by the superplastic forming of unstabilized Bi_2O_3, followed by the diffusion of one of the many known stabilizing elements[15] to retain the δ-Bi_2O_3 phase at room temperature. Second, Bi_2O_3 is a good model ceramic for other allotropic ceramics such as ZrO_2, HfO_2, or SiC, for which transformation superplasticity is experimentally more difficult, because of the higher transformation temperatures and higher creep strengths in the high-temperature phase.

The present paper reports on the transformation-mismatch plasticity of pure Bi_2O_3 that occurs during thermal cycling between two of its allotropic phases. This report differs from the above-reviewed studies on Bi_2O_3 in two important ways: first, strain increments are demonstrated over multiple thermal cycles; and second, deformation is conducted in tension (which is a necessary condition to demonstrate superplasticity). Furthermore, the measurements are compared with predictions from existing models of transformation superplasticity.

II. Experimental Procedures

Electronic-grade Bi_2O_3 powders (99.9995% pure, mean particle size of 45 μm; Metal Specialties Products, Fairfield, CT) were sieved to −45 μm, ground with 6 wt% deionized water for 5 min, and uniaxially pressed at 65 MPa for 90 s in a rectangular die. The resulting bars were dried, cold isostatically pressed at 275 MPa for 10 min, and sintered in air for 24 h on an Al_2O_3 refractory brick at 700°C to the approximate dimensions of 57 mm × 17 mm × 8 mm (heating and cooling rates of 5°C/min). The sintered bars were ground to overall dimensions of 50.1 mm × 16.7 mm × 2.5 mm, and a rectangular gauge section was machined to a length of 16.7 mm, a width of 4.6 mm, and a sharp shoulder radius of <1 mm. Finally, the tensile specimens were hand-polished with 600 grit SiC paper to remove any small chips that may have been incurred during machining and ultrasonically cleaned in acetone before testing.

As reported in another publication,[8] a servo-mechanical testing machine was used in a first series of experiments on six specimens (labeled S1–S6). Before thermal cycling, tensile isothermal creep rates were measured at a temperature of 760° ± 5°C in the δ-Bi_2O_3 phase, and these data are used later in the present paper. However, the servo-mechanical machine had difficulties maintaining a constant load during the allotropic transformation; therefore, the thermal cycling results[16] were considered unreliable and are not reported here.

A creep apparatus that ensured constant-tensile-load conditions was used for nine additional specimens, labeled C1–C9. Specimen elongation was calculated from measurements of the load-train travel outside the hot zone. The specimen temperature was determined with a thermocouple that was located at the center of the gauge length and a few millimeters away from the specimen

D. S. Wilkinson—contributing editor

Manuscript No. 189360. Received May 13, 1999; approved April 24, 2000.
Research sponsored by the U.S. Army Research Office (under Contract No. DAAH004-95-1-0629).
Presented in part at the 100th Annual Meeting of the American Ceramic Society, Cincinnati, OH, May 5, 1998 (Creep and Creep-Rupture Poster Session, Paper No. SXVIIP-032-98).
Based in part on the thesis submitted by author JLG for the M.S. degree in Materials Science and Engineering, Northwestern University, 1998.
[*]Member, American Ceramic Society.
[†]Author to whom correspondence should be addressed.
[‡]Now with Tempco Electric Heater Corp., Wood Dale, IL 60191.

surface, to avoid chemical reaction. After equilibrating at 760° ± 5°C with minimal stress (<0.05 MPa), the specimens first were deformed in tension under isothermal conditions while maintaining the temperature within ±1°C, as we have reported elsewhere.[8] Specimens C1, C4, and C7–C9 subsequently were thermally cycled at a rate of 5°C/min in the temperature range of 600°–760°C (±5°C) under constant tensile loads, which produced initial stresses in the range of 0.11–0.55 MPa (see Table I). Except for specimens C1 and C4, fracture occurred either during cycling, or just after cycling but before a steady-state isothermal creep rate could be measured. Specimen C1 was further subjected to tensile creep under isothermal and thermal cycling conditions for a second stress level. For all experiments, the specimen stress was calculated using the cross-sectional area that was determined from the instantaneous specimen length, assuming volume conservation and no necking.

The density of each sintered rectangular bar was measured before machining according to ASTM Standard C-373. Also, the density of the head and gauge sections of selected specimens were measured after mechanical testing. The average grain diameter of one sintered specimen with 98% relative density was determined using the Jeffries planimetric method,[17] after polishing to 0.3 μm alumina and thermal etching in the α-Bi_2O_3 phase for 1 h in air at 700°C. The mechanically tested specimens were too weak to be polished and were not examined for grain size.

III. Results

The average as-sintered α-Bi_2O_3 grain size was 13 μm, and the as-sintered bulk relative densities varied over the range of 97.6%–99.9% for all specimens that were subjected to thermal cycling (see Table I). For comparison, relative densities of 85%–97% and grain sizes of 9–17 μm were achieved by Johnson *et al.*[9] for Bi_2O_3 specimens that were hot-pressed at 650°C for 45 min under a stress of 21 MPa.

Figure 1(a) shows the measured displacement and temperature history for specimen C4. On heating under minimal stress, the measured displacement is due to the load-train thermal expansion and specimen phase transformation at 680°C. During subsequent isothermal creep at 760°C and a stress of 0.31 MPa, deformation is solely due to specimen creep. Then, on thermal cycling under load, specimen plastic deformation is superimposed to recoverable thermal expansion and contraction of the load train. Finally, during the subsequent isothermal creep, displacement is again due to specimen deformation only. The displacement curve shows discontinuities that correspond to the specimen phase transformations (expansion on heating and contraction on cooling).

Enlarged views of the strain history at the first transformations on cooling and heating under stress are given in Figs. 1(b) and (c), respectively. For cooling, the onset of the phase transformation is well-defined at the last data point before the transformation discontinuity at time $t_{1,c}$. The end of the transformation, at time $t_{2,c}$, is located at the corresponding deviation from the best-fit line of the cooling strain curve after the transformation. Then, the transformation time is $\Delta t_c = t_{2,c} - t_{1,c}$. A similar procedure has been used for the heating portion of the strain curve, to determine the transformation time on heating ($\Delta t_h = t_{2,h} - t_{1,h}$), as illustrated in Fig. 1(c). The average transformation times for all thermally cycled specimens are $\Delta t_c = 138 \pm 124$ s (35 cooling data points) and $\Delta t_h = 278 \pm 35$ s (32 heating data points). Transformation temperatures T_c and T_h, at the start of the transformations at $t_{1,c}$ and $t_{1,h}$, respectively, are marked with dots on Fig. 1(a) and are reproducible from cycle to cycle. The average values for all specimens are $T_c = 648° \pm 24$°C and $T_h = 697° \pm 7$°C.

Thermal and allotropic expansion and contraction are recoverable over a full thermal cycle; therefore, the strain accumulated from one temperature maximum to the next ($\Delta\epsilon_1$) in Fig. 1(a) (or from one temperature minimum to the next ($\Delta\epsilon_2$)) is solely due to plastic deformation of the specimen. Figure 2 shows the stress dependence of the average strain accumulated over a complete thermal cycle ($\Delta\epsilon_{tot}$), which is determined as the average of all measured values for $\Delta\epsilon_1$ and $\Delta\epsilon_2$ for a given specimen, except for the first maximum and minimum, which correspond to the first cooling ramp (at times of 15 and 17 ks, respectively, in Fig. 1(a)) for which a dynamic thermal equilibrium had not been attained in the load train. The standard deviation for each test was used as the error bar in Fig. 2. A point was placed at the origin because no strain increments are expected at zero stress, assuming no thermal ratcheting. The slope of the best-fit line in Fig. 2 is $\Delta\epsilon_{tot}/\sigma = 78$ GPa^{-1} (which corresponds to a total strain increment of 7.8% after a full cycle at a stress of 1 MPa).

Figure 3 shows a photograph of specimen C4 before and after deformation to fracture to a total strain of 28%, of which 11% was accumulated during the isothermal creep segments before and after thermal cycling and 17% during cycling (see Table I). The specimen exhibited partial necking in the gauge length but fractured at the sharp corner at the end of the gauge section, as did most of the specimens used in the present study. A few specimens fractured near the center of the gauge length, as a result of stable crack growth, which was observed visually during cycling after 1–6 cycles. Some of the cracks and the fracture at the head of specimen C4 in Fig. 3 occurred on rapid cooling after fracture and during extraction of the specimen from the pull-heads.

Table I gives, for selected specimens, the porosity measured after cycling, which increased from the initial porosity by ~1% for specimens C7 and C8 and ~4.6% for specimen C4. Furthermore, two creep specimens[8] showed a porosity increase of ~1.5% after creep deformation at 760°C and the transformations that are associated with the initial heating and final cooling with minimal applied stress. Unlike metals, for which porosity is created by cavitation only in the deforming gauge section, no significant difference was observed in the porosity that was created in the head and gauge of the Bi_2O_3 specimens, which indicated that the increased porosity is mostly due to thermal cycling (most probably by internal cracking), rather than deformation-induced cavitation.

IV. Discussion

(1) Transformation-Mismatch Plasticity Strains

The total plastic strain increment $\Delta\epsilon_{tot}$ accumulated after each thermal cycle shown in Fig. 2 is the sum of two contributions:

$$\Delta\epsilon_{tot} = \Delta\epsilon_{creep} + \Delta\epsilon_{tp} \tag{1}$$

where $\Delta\epsilon_{creep}$ is the creep strain accumulated during the cycle while the specimen is not undergoing a transformation and $\Delta\epsilon_{tp}$ is

Table I. Summary of Thermal Cycling Experiments

Specimen	Initial stress (MPa)	Total number of cycles	Initial porosity (%)	Final porosity (%)	Average strain per cycle (%)	Cumulative cycling strain (%)	Total fracture strain (%)
C1	0.11	6	0.1		0.39	2.2	
	0.21	10			1.30	7.0	12.2
C9	0.31	4.5	0.8		2.67	10.1	15.2
C4	0.31	6	0.6	5.2	2.81	16.9	28.4
C7	0.40	4.5	2.4	3.6	3.04	12.8	21.6
C8	0.55	2.5	2.0	2.7	3.90	8.6	10.3

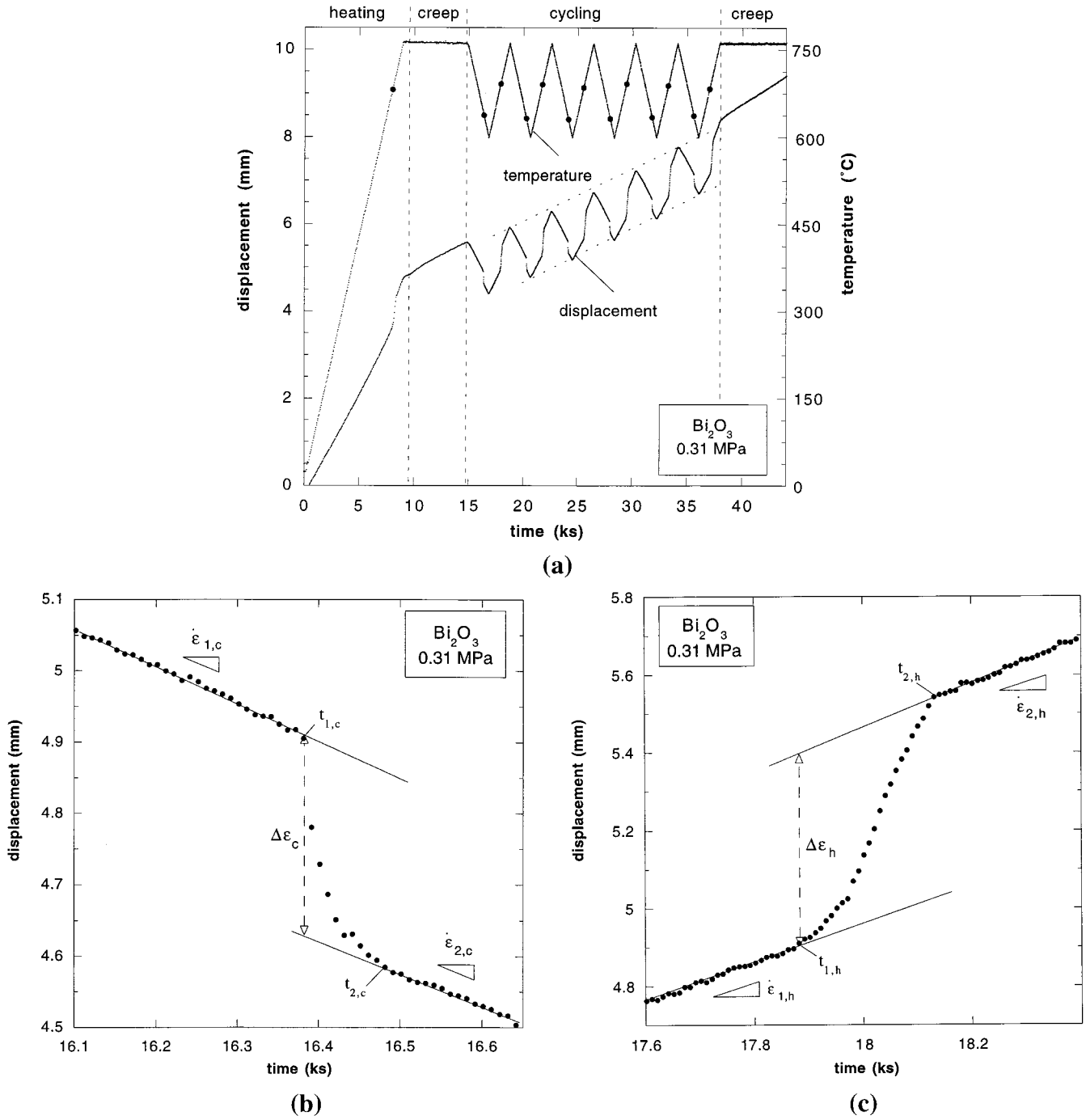

Fig. 1. (a) Displacement and temperature history of specimen C4, showing heating under minimal stress and creep at 0.31 MPa (thermal cycling creep, preceded and followed by isothermal creep). Temperatures at which the specimen showed an acceleration of strain due to phase transformation are marked with dots. Detailed displacement history of specimen C4 for (b) the first transformation on cooling and (c) the subsequent transformation on heating also is shown.

the plastic strain increment due to transformation plasticity accumulated during both heating and cooling transformations. To compare our results to transformation-superplasticity theory, $\Delta\epsilon_{tp}$ must be determined first. The first method consists of calculating $\Delta\epsilon_{creep}$ from the experimentally derived creep constitutive equation and subtracting $\Delta\epsilon_{creep}$ from the measured value of $\Delta\epsilon_{tot}$ to find $\Delta\epsilon_{tp}$ according to Eq. (1). A second method takes advantage of the discontinuities in the strain curve that occur on transformation during the cooling and heating portions of a thermal cycle (see Figs. 1(b) and (c)) to determine $\Delta\epsilon_{tp}$ directly. Both methods are described in more detail in the following sections.

(A) Creep-Strain Method: The creep strain $\Delta\epsilon_{creep}$ accumulated outside the transformation range can be calculated, based on the creep constitutive equation of δ-Bi_2O_3, as

$$\Delta\epsilon_{creep} = \int_{t_{2,h}}^{t_{1,c}} K\sigma^n \exp\left(-\frac{Q}{RT(t)}\right) dt \tag{2}$$

where K is the power-law constant, n the stress exponent, Q the activation energy, R the gas constant, and $T(t)$ the temperature history of the specimen in the δ-phase, which is present from $t_{2,h}$ to $t_{1,c}$. Creep in the δ-phase is many orders of magnitude faster than in any of the low-temperature phases;[7] therefore, creep between $t_{2,c}$ and $t_{1,h}$ when δ-Bi_2O_3 was not present is assumed to be negligible. Here, values of $K = 6.0 \times 10^3$ $MPa^{-1/3}\cdot s^{-1}$ and $n =$

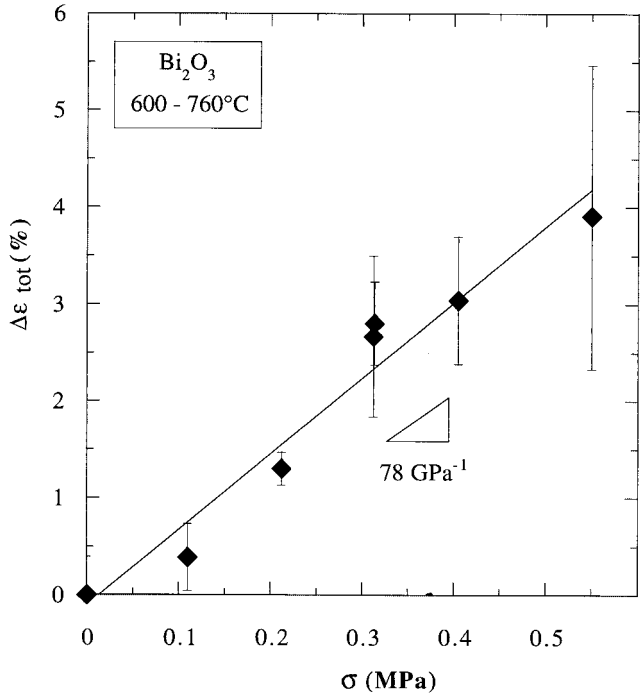

Fig. 2. Average total strain increment, measured after each thermal cycle, as a function of the applied stress (standard deviations are used as error bars).

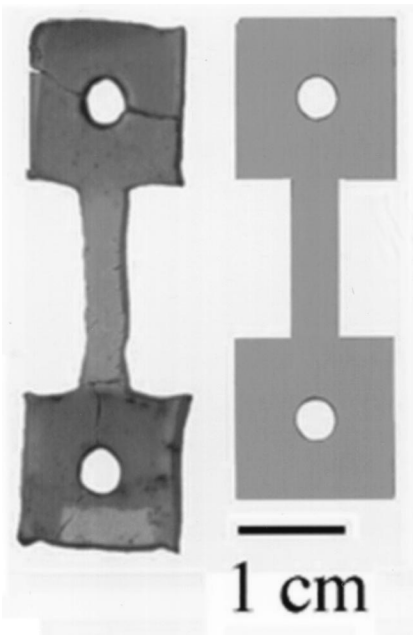

Fig. 3. Photograph of specimen C4 before testing (right) and after testing (left) (strain to failure of 28%).

1.3 have been used; these values were determined from creep data measured at 760°C for the stress range of 0.1–0.8 MPa on δ-Bi_2O_3 specimens C1–C9 before and after thermal cycling, as well as specimens S1–S6 before temperature cycling, as we have described in another work.[8] The average activation energy of Q = 165 kJ/mol was used; this value was determined from two experiments in the range of 680°–760°C for a stress of 0.3 MPa, giving Q_1 = 130 kJ/mol and Q_2 = 200 kJ/mol.[8] That study showed that no significant difference was observed in the measured isothermal creep before and after multiple cycles under load about the phase transformation; therefore, here, we are justified to use the average materials parameters K, Q, and n to calculate the creep accumulated during the thermal cycles from Eq. (2). Integration of Eq. (2) was performed numerically, using time intervals of 1.2 s (which correspond to 0.1°C), based on the experimental temperature profiles, which varied slightly between tests. Using the resulting values of $\Delta\epsilon_{creep}$, the transformation-plasticity strain increment $\Delta\epsilon_{tp}$ was determined from Eq. (1) and is shown in Fig. 4 as a function of stress for all thermal cycling experiments (the error bars in Fig. 4 represent extreme values that were calculated using Q_1 and Q_2).

(B) Strain-Jump Method: For Bi_2O_3 with a positive relative mismatch in specific volume ($\Delta V/V$) on heating, the total uniaxial strain on heating through the phase transformation ($\Delta\epsilon_h$) is

$$\Delta\epsilon_h = \frac{1}{3}\left(\frac{\Delta V}{V}\right) + \Delta\epsilon_{tp,h} \tag{3}$$

where $\Delta\epsilon_{tp,h}$ is the transformation plasticity strain accumulated on heating, which is assumed to be completely developed over the transformation time Δt_h. Similarly, the total uniaxial strain on cooling through the phase transformation ($\Delta\epsilon_c$) is

$$\Delta\epsilon_c = -\frac{1}{3}\left(\frac{\Delta V}{V}\right) + \Delta\epsilon_{tp,c} \tag{4}$$

where the specific volume decrease during the Bi_2O_3 phase change on cooling acts to counter the positive transformation plasticity strain increment ($\Delta\epsilon_{tp,c}$). Thermal expansion strains over the transformation range are neglected in the previous two equations, because of the narrow transformation temperature range.

Then, the total transformation-plasticity strain increment accumulated over one complete thermal cycle ($\Delta\epsilon_{tp}$) is the sum of the transformation plasticity strains accrued during the heating and cooling portions of the cycle:

$$\Delta\epsilon_{tp} = \Delta\epsilon_{tp,c} + \Delta\epsilon_{tp,h} \tag{5}$$

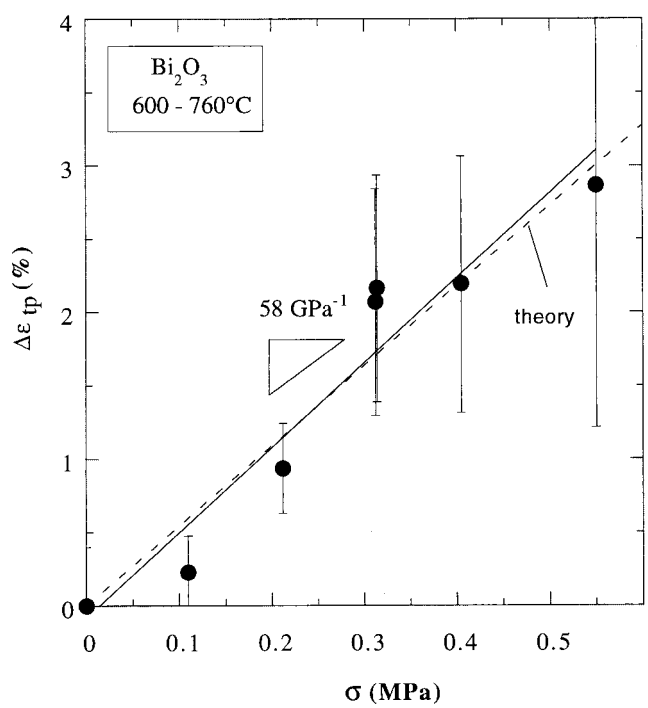

Fig. 4. Dependence on applied stress (σ) of the average strain increment due to transformation-mismatch plasticity accumulated after one thermal cycle ($\Delta\epsilon_{tp}$), as calculated by subtracting the creep contribution from the total measured strain increment (Eq. (1)). Error bars are from correction using two activation-energy values. Theoretical line is calculated from Eqs. (7) and (8), using the model by Greenwood and Johnson.[22]

Substitution of Eqs. (3) and (4) into Eq. (5) yields

$$\Delta\epsilon_{tp} = \Delta\epsilon_c + \Delta\epsilon_h \tag{6}$$

Thus, experimental determination of $\Delta\epsilon_c$ and $\Delta\epsilon_h$ allows for calculation of the strain increment from transformation plasticity ($\Delta\epsilon_{tp}$). As shown in Fig. 1(b) for the displacement (or strain) curve on cooling, $\Delta\epsilon_c$ is taken at time $t_{1,c}$ as the strain difference between the two extrapolated lines $\dot{\epsilon}_{1,c}$ and $\dot{\epsilon}_{2,c}$. A similar procedure was used for the heating portion of the strain curve to determine $\Delta\epsilon_h$, as illustrated in Fig. 1(c). Figure 5 shows that a linear relationship exists between the applied stress σ and the average transformation plasticity strain increment $\Delta\epsilon_{tp}$, calculated from Eq. (6) with $\Delta\epsilon_c$ and $\Delta\epsilon_h$ determined by the above-described method, using the standard deviation for error bars. Within the substantial experimental error, there is good agreement between the plasticity strains obtained by the creep-strain method (Fig. 4), which is used in most transformation-plasticity studies of metals (see, for example, the work of Dunand and co-workers[18–20]), and the strain-jump method (Fig. 5), which is more rarely used in metals.[21]

(C) Comparison with Literature Data: Table II gives a summary of transformation-mismatch plasticity studies on Bi_2O_3 and Bi_2O_3-based ceramic systems. Comparison with our study is difficult for several reasons. First, all the past research was performed in compression, whereas our study was performed in tension. Experimental errors that are linked to cavitation and cracking in tension and to pore densification, platten friction, and sample barreling in compression are different. Second, except for Smyth *et al.*,[11] who reported strains accumulated over four cycles for hypereutectoid Bi_2O_3–8% Sm_2O_3, all other studies failed to obtain any strain after more than a half-cycle (i.e., on initial heating).

In the only existing study that has been performed on pure Bi_2O_3, Johnson *et al.*[9] reported a transformation-plasticity strain increment per unit stress ($\Delta\epsilon_{tp}/\sigma$) of 190 GPa^{-1} for specimens with a density of 94% and a grain size of 10 μm heated at a rate of 5°C/min. The value found in the present study ($\Delta\epsilon_{tp}/\sigma$ = 45–58 GPa^{-1}, Figs. 4 and 5) is smaller by a factor of ~7, considering only the heating half-cycle. However, other results by Johnson *et al.*[9] indicate that the transformation strains decrease as the grain size increases (a factor-of-5 difference was observed between specimens with grain sizes of 9 and 17 μm), the heating rate increases (by a factor of 3, from 2.5°C/min to 14°C/min), and the porosity increases (by a factor of 2, from 4% to 9%); thus, their $\Delta\epsilon_{tp}/\sigma$ values span a very wide range (40–360 GPa^{-1}).

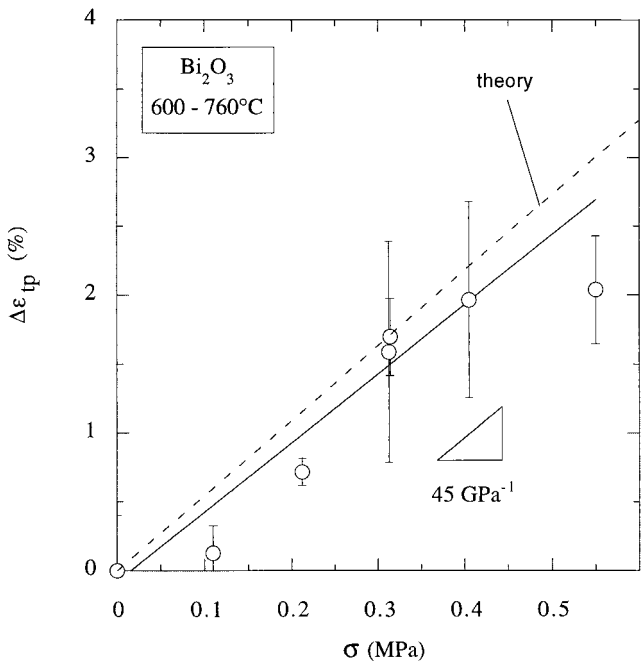

Fig. 5. Dependence on applied stress (σ) of the average strain increment due to transformation-mismatch plasticity accumulated after one thermal cycle ($\Delta\epsilon_{tp}$), as determined from strain jumps (Eq. (6)). Standard deviations were used for the error bars. Theoretical line (dashed) is calculated from Eqs. (7) and (8), using the model by Greenwood and Johnson.[22]

The two main discrepancies between the results by Johnson *et al.*[9] and our findings are (i) their high transformation-plasticity strain values on initial heating and (ii) their lack of transformation plasticity on cooling and subsequent cycling. The first discrepancy can be explained, in part, by the higher porosity of their specimens, which probably densified during the phase transformation, as well as possibly by large primary creep contributions during and after transformation (they reported decreases of two orders of magnitude in the creep rate of the low-temperature phase after cycling). The lack of subsequent transformation strain was explained by Johnson *et al.*[9] by grain growth that occurs in the δ-phase, which decreased the strain that was produced during transformation by a grain-size-sensitive deformation mechanism. However, Vilette and Kampe[7] reported that, for δ-Bi_2O_3 with 9 μm grains, dislocation creep (which is grain-size independent) was the main deformation mechanism at 750°C for stresses as low as 1 MPa, well below the maximum stress of 6 MPa used by Johnson *et al.*[9] Thus, the reason for the absence of repeatable transformation-plasticity strains in that study is unknown, especially since we were able to measure repeatable, consistent strains increments after each thermal cycle.

(D) Comparison with Model: Greenwood and Johnson[22] studied pure allotropic metals that were subjected to thermal cycling around the phase transformations and derived an equation for the strain increment that was produced by transformation-mismatch plasticity after each crossing of the allotropic temperature:

$$\Delta\epsilon_{tp,i} = \frac{2}{3}\left(\frac{\Delta V}{V}\right)\left(\frac{\sigma}{\sigma_{o,i}}\right)\left(\frac{5n}{4n+1}\right) \tag{7}$$

where the subscript i can be "h" (for heating) or "c" (for cooling), n is the stress exponent of the weakest phase deforming by creep, and σ_o is the allotropic internal stress (which is averaged over the transformation time and specimen volume). The data in Figs. 4 and 5 can be fitted with Eq. (7) to an average internal stress of σ_o = 1.9–2.4 MPa, assuming that both transformations contribute the same strain (this assumption is discussed later) and using a value of $\Delta V/V$ = 6.9% for the $\alpha \rightleftarrows \delta$ transformation.[6] For the stress exponent, we used the dislocation-creep value of n = 3.5, which was determined from creep data by Vilette and Kampe[7] for stresses in the range of ~0.9–2.5 MPa but was valid for stresses as low as 0.3 MPa.[8] Given the high value of the average internal stress, the stress exponent for diffusional creep—n = 1.3, which is valid over a lower range of stresses (0.1–0.8 MPa)[8]—cannot be used in Eq. (7). The linear relationship between applied stress and strain increment given by Eq. (7) is valid only when the σ value is less than approximately half of the σ_o value.[19,20,23] This condition is fulfilled in our case, because the largest σ value is 0.55 MPa.

By considering creep relaxation of internal stresses during the transformation, Greenwood and Johnson[22] showed that the internal stress $\sigma_{o,i}$ can be expressed as

$$\sigma_{o,i} = \left\{\frac{2}{3}\left(\frac{\Delta V}{V}\right)\left(\frac{1}{\Delta t_i}\right)\left[\frac{\exp\left(\frac{Q}{RT_i}\right)}{K}\right]\right\}^{1/n} \tag{8}$$

where Δt_i and T_i are the average duration and temperature of the phase transformations, respectively. Thus, substitution of Eq. (8) into Eq. (7) gives a predictive expression for the transformation-plasticity strains per unit stress ($\Delta\epsilon_{tp,i}$), from which the value for a full cycle can be calculated through Eq. (5) and compared with the measured values of $\Delta\epsilon_{tp}/\sigma$ = 45–58 GPa^{-1}. Quantitative evaluation of Eqs. (7) and (8) requires three material parameters that are related to creep of the weakest δ-phase (K, Q, and n) and three parameters that are related to the transformations (Δt_i, T_i, and $\Delta V/V$). The average power-law creep parameters of δ-Bi_2O_3 can be

Table II. Summary of Transformation Plasticity Studies on Bi_2O_3 and Bi_2O_3-Based Ceramics

Material	Initial grain size (μm)	Initial porosity (%)	Temperature range (°C)	Stress range (MPa)	Maximum strain per cycle,† $\Delta\epsilon_{tp}$	Strain per cycle† and unit stress, $\Delta\epsilon_{tp}/\sigma$ (GPa^{-1})	Reference
Bi_2O_3	13	0–2.5	600–760	0.1–0.6	0.03	52	Present study
Bi_2O_3	9–17	3–15	700–760	0.3–5.8	1.15	190	Johnson *et al.*[9]
Bi_2O_3–Sm_2O_3							
Hypoeutectoid	9–20	0	660–750	0.7–5.9	0.62	120	Smyth *et al.*[11]
Hypereutectoid	12	0	660–750	1.4–5.4	0.55	135	Smyth *et al.*[11]
Bi_2WO_6	3–14	6	835–935	0.1–0.6	0.75	580–900	Johnson *et al.*[9] and Winger *et al.*[12]
Bi_2MoO_6	5		625–725	1.8–6.8	0.41	65	Winger *et al.*[12]

†No strain was measured in the cooling portion of the cycle, except in the present study.

determined from data by Vilette and Kampe[7] as $K = 7.425 \times 10^6$ $MPa^{-1/3}\cdot s^{-1}$, $Q = 210$ kJ/mol, and $n = 3.5$. We have used the measured average transformation times Δt_c and Δt_h and the average transformation temperatures T_c and T_h. Finally, again, for the allotropic volume mismatch, we have used the value $\Delta V/V = 6.9\%$, which has been reported for the $\alpha \rightleftarrows \delta$ transformation by Levin and Roth.[6] The parameters Δt_i, T_i, and $\Delta V/V$ are discussed in more detail in the next sections.

With the above-given materials parameters, Eqs. (7) and (8) give values of $\sigma_{o,h} = 1.5$ MPa and $\Delta\epsilon_{tp,h}/\sigma = 35$ GPa^{-1} for the transformation on heating and $\sigma_{o,c} = 2.8$ MPa and $\Delta\epsilon_{tp,c}/\sigma = 19$ GPa^{-1} for the transformation on cooling. Thus, for a full cycle, the strain per cycle is given as $(\Delta\epsilon_{tp,h} + \Delta\epsilon_{tp,c})/\sigma = 54$ GPa^{-1}. This value, which is found using experimentally determined parameters without any adjustable parameters, is consistent with the experimental values $\Delta\epsilon_{tp}/\sigma = 45$–$58$ GPa^{-1} (see Figs. 4 and 5). Similarly, the average internal stresses for both transformations is $(\sigma_{o,c} + \sigma_{o,h})/2 = 2.2$ MPa, which is in good agreement with the value $\sigma_o = 1.9$–2.4 MPa calculated earlier under the rough approximation that the transformations on heating and cooling were the same.

We conclude that, despite the large experimental errors that are present in our measurements, the measured strain increments obtained during thermal cycling of Bi_2O_3 can be predicted quantitatively, using the transformation-mismatch plasticity theory developed by Greenwood and Johnson[22] for pure, creeping materials.

(2) Transformation Temperatures and Times

Many authors[5,6,24–26] have reported that monoclinic α-Bi_2O_3 transforms to face-centered cubic (fcc) δ-Bi_2O_3 at 730° ± 5°C on heating. Levin and Roth[6] showed that the transformation can follow any of three paths on cooling at a rate of 7°C/min, which is comparable to that used in the present study: (i) transformation to stable, monoclinic α-Bi_2O_3 at 700°C; (ii) transformation to metastable, tetragonal β-Bi_2O_3 at ~650°C; or (iii) transformation to metastable, body-centered cubic (bcc) γ-Bi_2O_3 at ~640°C. The $\delta \rightarrow \alpha$ transformation occurred if the δ-phase was not previously heated above ~745°C, whereas either the $\delta \rightarrow \beta$ or $\delta \rightarrow \gamma$ transformation could occur for specimens that were heated above ~775°C. On further cooling, γ-Bi_2O_3 could be retained to room temperature, whereas β-Bi_2O_3 transformed to α-Bi_2O_3 at ~550°C. However, if β-Bi_2O_3 was reheated, the $\beta \rightarrow \delta$ transformation occurred at ~660°C; for γ-Bi_2O_3, $\gamma \rightarrow \alpha$ and $\alpha \rightarrow \delta$ transformations were observed at 625° and 730°C, respectively, on heating. Harwig and Gerards[5] determined similar results, with a few variations: the $\delta \rightarrow \alpha$ transformation was observed at ~640°C (instead of 700°C); direct $\gamma \rightarrow \delta$ transformation was observed at ~660°C (instead of the $\gamma \rightarrow \alpha \rightarrow \delta$ transformations at 625° and 730°C); the $\gamma \rightarrow \alpha$ and $\beta \rightarrow \alpha$ cooling transformations could occur over broad temperature ranges of 639°–500°C and 650°–330°C, respectively. The probability for the $\delta \rightarrow \gamma$ and $\delta \rightarrow \beta$ transformations was approximately the same, with no data for the $\delta \rightarrow \alpha$ transformation.

The above-described literature survey indicates that many transformation paths are possible for our experiments, assuming that the applied stress has no effect on the transformations. Although only the $\alpha \rightarrow \delta$ transformation is expected on initial heating from room temperature to 760°C, all three transformations—$\delta \rightarrow \alpha$, $\delta \rightarrow \beta$, or $\delta \rightarrow \gamma$—are possible on cooling from 760°C to 600°C, with or without subsequent $\beta \rightarrow \alpha$ and $\gamma \rightarrow \alpha$ transformations. On subsequent heating from 600°C to 760°C, the low-temperature phase is expected to transform back to the δ-phase. Thus, in our case, cycling occurred between the δ-phase and any of the three low-temperature phases (according to $\delta \rightleftarrows \alpha$, β, or γ), with no systematic preference for a particular phase and with possible intermediate transformations.

Examination of our data for transformation temperatures on cooling indicates that the average value $T_c = 648° \pm 24$°C results from data clustered around two separate temperatures: twenty-six data points with $T_c = 638° \pm 16$°C and nine data points with $T_c = 683° \pm 9$°C. All six specimens first exhibited the lower transformation temperature; four specimens showed the higher transformation temperature after 2–7 cycles. The lower transformation temperature can be assigned to $\delta \rightarrow \beta$ or $\delta \rightarrow \gamma$ transformations, according to the work of Levin and Roth[6] (and/or to the $\delta \rightarrow \alpha$ transformation, according to Harwig and Gerards[5]), whereas the higher transformation temperature can be assigned to the $\delta \rightarrow \alpha$ transformation.[6] The transformation temperature on heating ($T_h = 697° \pm 7$°C, which, unlike the cooling temperature, showed no systematic variation), does not correspond to any of the values reported by Harwig and Gerards[5] and Levin and Roth.[6] However, it is, within error, equal to the transformation temperature that is measured on initial heating without stress (684° ± 6°C for five data points) and, thus, can be assigned to the $\alpha \rightarrow \delta$ transformation. The discrepancy between these temperatures (~690°C) and the literature values (~730°C) remains unexplained.

The transformation times on cooling were correlated with the transformation temperature: their average value is $\Delta t_c = 78 \pm 14$ s for the cycles with the lower transformation temperature and $\Delta t_c = 310 \pm 142$ s for those with the higher transformation temperature. As for transformation temperatures, there is no systematic variation for the transformation times on heating ($\Delta t_h = 278 \pm 35$ s). Thus, transformations on both heating and cooling near 690°C ($\delta \rightleftarrows \alpha$) are much longer than the cooling transformation near 640°C ($\delta \rightarrow \alpha$, β, or γ). Two mechanisms can explain this difference. First, the transformation enthalpies for the $\delta \rightarrow \gamma$ and $\delta \rightarrow \beta$ transformations (21 and 22 kJ/mol, respectively) are less than that for the $\delta \rightarrow \alpha$ transformation (30 kJ/mol).[5] Second, on cooling, the specimens glowed brightly during the exothermic transformation. This phenomenon is typical of recalescence on undercooling and also was observed by Gattow and Schröder,[27] who reported that the temperature of their Bi_2O_3 specimen briefly increased from 647°C just before transformation to 712°C at the recalescence maximum (our specimens were not in direct contact with the thermocouple; therefore, we did not measure the optically visible temperature jumps). Thus, a specimen that has been undercooled at ~640°C and then suddenly heated to the transformation temperature by recalescence will radiate against much-cooler surroundings and transforms more rapidly than a specimen that transforms at ~690°C with minimum or no undercooling (or superheating).

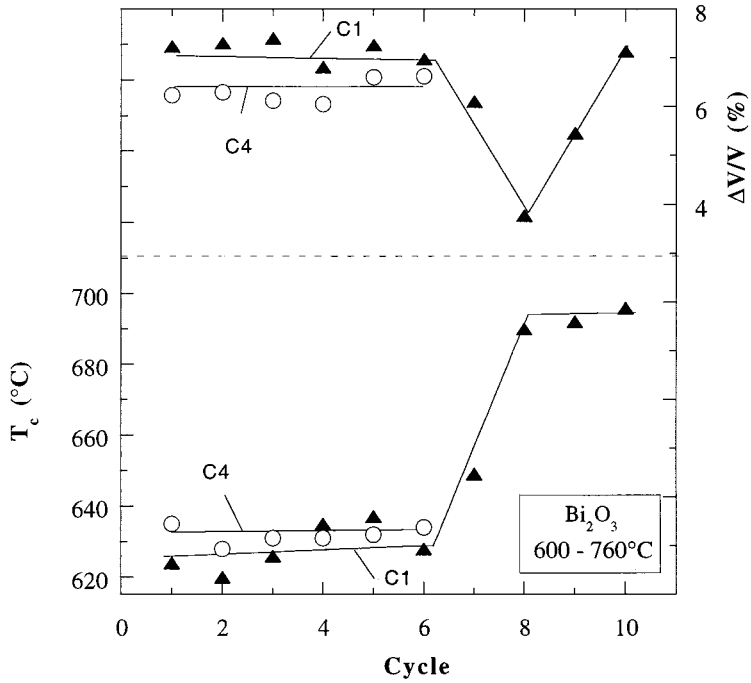

Fig. 6. Temperature for onset of transformation on cooling (T_c) and calculated allotropic volume mismatch ($\Delta V/V$, Eq. (10)), as a function of cycle number for tests on specimens C1 and C4.

(3) Transformation-Volume Mismatch

As shown previously, the transformation-plasticity contributions on heating and cooling are different:

$$\Delta\epsilon_{tp,c} = k\Delta\epsilon_{tp,h} \tag{9}$$

where $k = 19/35 = 0.55$ in the present case. Substitution of Eqs. (3) and (4) into Eq. (9) gives

$$\frac{\Delta V}{V} = \frac{3}{k+1}(k\Delta\epsilon_h - \Delta\epsilon_c) \tag{10}$$

which allows the determination of the transformation-volume mismatch from measured values of k, $\Delta\epsilon_h$, and $\Delta\epsilon_c$. The average value of the transformation mismatch determined using Eq. (10) with twenty-seven individual measurements of $\Delta\epsilon_h$ and $\Delta\epsilon_c$ for specimens in Table I is $\Delta V/V = 6.5\% \pm 1.0\%$. This value is in good agreement with the value of $\Delta V/V = 6.9\%$ for the $\delta \rightleftarrows \alpha$ transformation[6] and is significantly larger than the $\Delta V/V$ values of 2.1% and 4.5% for the $\delta \rightleftarrows \beta$ and $\delta \rightleftarrows \gamma$ transformations, respectively.[6] This result indicates that the $\delta \rightleftarrows \alpha$ transformation was the most prevalent, with possible intermediate phases.

The onset transformation temperature on cooling (T_c) and the associated allotropic volume mismatch ($\Delta V/V$) calculated from Eq. (10) are shown in Fig. 6 for tests on specimens C1 and C4. During the first six thermal cycles in both specimens, the values of T_c and $\Delta V/V$ were constant: ~630°C and ~6.5%, respectively. The temperature corresponds to any of the $\delta \rightarrow \alpha$, β, or γ transformations, whereas the allotropic volume mismatch corresponds to the $\delta \rightleftarrows \alpha$ transformation. Specimen C1, which was subjected to an additional four cycles, showed a transition on cycle 7 and a new equilibrium for cycles 8–10 at $T_c \approx 680$°C, which is indicative of the $\delta \rightarrow \alpha$ transformation. The value of $\Delta V/V$ varied between 4% (which was indicative of the $\delta \rightleftarrows \gamma$ transformation), and 7% (which was indicative of the $\delta \rightleftarrows \alpha$ transformation).

V. Conclusions

Bismuth sesquioxide (Bi_2O_3) specimens were subjected to a constant tensile stress and thermally cycled between the high-temperature, face-centered cubic δ-phase and one or more of the low-temperature phases (monoclinic α-Bi_2O_3, tetragonal β-Bi_2O_3, or body-centered cubic γ-Bi_2O_3). Because of the mismatch in specific volume between these phases, the phase transformations created internal stresses. Their relaxation was biased by the applied stress, which resulted in a macroscopic strain increment after a complete thermal cycle. These strain increments were proportional to the applied stress in the measured range of 0.11–0.55 MPa, as predicted from the model for transformation-mismatch plasticity by Greenwood and Johnson.[22] The measured slope, which was ~52 GPa^{-1} (which corresponds to a strain increment of 5.2% per cycle at a stress of 1 MPa), is quantitatively consistent with the theoretical predictions.

Reproducible strain increments were achieved over as many as ten thermal cycles, and a total tensile strain as high as 28% was accumulated before fracture from both isothermal creep and transformation plasticity. Although many metals have been reported to exhibit tensile strain increments because of transformation-mismatch plasticity, the present study is the first documented case for a ceramic. Total tensile elongations of >100% on repeated cycling (which are needed to formally claim transformation superplasticity and are observed routinely in metals) should be attainable in Bi_2O_3 in the future by inhibiting cracking and using specimens with smoother gauge profiles, thus minimizing stress concentrations near the specimen head.

Acknowledgment

The authors gratefully acknowledge useful discussions with C. Schuh (Northwestern University).

References

[1]T. G. Nieh, J. Wadsworth, and O. D. Sherby, *Superplasticity in Metals and Ceramics*. Cambridge University Press, Cambridge, U.K., 1997.

[2]T. G. Nieh, J. Wadsworth, and F. Wakai, "Recent Advances in Superplastic Ceramics and Ceramic Composites," *Int. Mater. Rev.*, **36**, 146–61 (1991).

[3]D. C. Dunand and B. Derby, "Creep and Thermal Cycling"; pp. 191–214 in *Fundamentals of Metal-Matrix Composites*. Edited by S. Suresh, A. Mortensen, and A. Needleman. Butterworth–Heinemann, Boston, MA, 1993.

[4]D. C. Dunand, "Transformation Superplasticity in Metals, Alloys and Composites"; pp. 1821–30 in *International Conference on Thermomechanical Processing of Steels and Other Materials*. TMS, Warrendale, PA, 1997.

[5]H. A. Harwig and A. G. Gerards, "The Polymorphism of Bismuth Sesquioxide," *Thermochim. Acta*, **28**, 121–31 (1979).

[6]E. M. Levin and R. S. Roth, "Polymorphism of Bismuth Sesquioxide, I. Pure Bi_2O_3," *J. Res. Natl. Bur. Stand., Sect. A*, **68A**, 189–95 (1964).

[7]A. Vilette and S. L. Kampe, "High-Temperature Plasticity of Cubic Bismuth Oxide," *J. Mater. Res.*, **11**, 1433–39 (1996).

[8]J. L. Grabowski and D. C. Dunand, "Tensile Creep Properties of δ-Bi_2O_3," *Scr. Mater*., in print.

[9]C. A. Johnson, R. C. Bradt, and J. H. Hoke, "Transformational Plasticity in Bi_2O_3," *J. Am. Ceram. Soc.*, **58** [1–2] 37–40 (1975).

[10]C. A. Johnson, J. R. Smyth, R. C. Bradt, and J. H. Hoke, "Transformational Superplasticity in Pure Bi_2O_3 and the Bi_2O_3–Sm_2O_3 Eutectoid System"; pp. 443–53 in *Deformation of Ceramic Materials*. Plenum, New York, 1975.

[11]J. R. Smyth, R. C. Bradt, and J. H. Hoke, "Transformational Superplasticity in the Bi_2O_3–Sm_2O_3 Eutectoid System," *J. Am. Ceram. Soc.*, **58** [9–10] 381–84 (1975).

[12]L. A. Winger, R. C. Bradt, and J. H. Hoke, "Transformational Superplasticity of Bi_2WO_6 and Bi_2MoO_6," *J. Am. Ceram. Soc.*, **63** [5–6] 291–94 (1980).

[13]H. L. Tuller and P. K. Moon, "Fast Ion Conductors: Future Trends," *Mater. Sci. Eng., B*, **1B**, 171–91 (1988).

[14]A. M. Azad, S. Larose, and A. Akbar, "A Review of Bismuth Oxide-Based Solid Electrolytes For Fuel Cells," *J. Mater. Sci.*, **29**, 4135–51 (1994).

[15]E. M. Levin and R. S. Roth, "Polymorphism of Bismuth Sesquioxide. II. Effect of Oxide Additions on the Polymorphism of Bi_2O_3," *J. Res. Natl. Bur. Stand., Sect. A*, **68A**, 197–206 (1964).

[16]J. L. Grabowski, "Transformation Superplasticity of Bi_2O_3"; M.S. Thesis. Dept. of Materials Science and Engineering, Northwestern University, Evanston, IL, 1998.

[17]H. E. Boyer and T. L. Gall (eds.), *Metals Handbook*, Desk Edition. ASM, Metals Park, OH, 1985.

[18]D. C. Dunand and C. M. Bedell, "Transformation-Mismatch Superplasticity in Reinforced and Unreinforced Titanium," *Acta Mater.*, **44**, 1063–76 (1996).

[19]P. Zwigl and D. C. Dunand, "Transformation Superplasticity of Zirconium," *Metall. Trans. A*, **29**, 2571–82 (1998).

[20]C. Schuh and D. C. Dunand, "Transformation Superplasticity of Titanium Aluminides," *Acta Mater.*, **46**, 5663–75 (1998).

[21]N. Furushiro, H. Kuramoto, Y. Takayama, and S. Hori, "Fundamental Characteristics of the Transformation Superplasticity in a Commercially-Pure Titanium," *Trans. Iron Steel Inst. Jpn.*, **27**, 725–29 (1987).

[22]G. W. Greenwood and R. H. Johnson, "Deformation of Metals Under Small Stresses During Phase Transformations," *Proc. R. Soc. London, A*, **283A**, 403–22 (1965).

[23]P. Zwigl and D. C. Dunand, "A Non-Linear Model for Internal Stress Superplasticity," *Acta Mater.*, **45**, 5285–94 (1997).

[24]H. A. Harwig, "On the Structure of Bismuth Sesquioxide: The α, β, γ and δ-Phase," *Z. Anorg. Allg. Chem.*, **444**, 151–66 (1978).

[25]H. A. Harwig and J. W. Weenk, "Phase Relations in Bismuth Sesquioxide," *Z. Anorg. Allg. Chem.*, **444**, 167–77 (1978).

[26]H. A. Harwig and A. G. Gerards, "Electrical Properties of the α, β, γ and δ Phases of Bismuth Sesquioxide," *J. Solid State Chem.*, **26**, 265–74 (1978).

[27]G. Gattow and H. Schröder, "Die Kristallstruckture der Hochtemperaturmodifikation von Wismut(III)-Oxid," *Z. Anorg. Allg. Chem.*, **318**, 176–89 (1962). □